Journal of Alloys and Compounds 508 (2010) 158–161

Contents lists available at ScienceDirect

Journal of Alloys and Compounds

journal homepage: www.elsevier.com/locate/jallcom

Growth and characterization of nonpolar *a*-plane ZnO films on perovskite oxides with thin homointerlayer

Yuan-Chang Liang

Institute of Materials Engineering, National Taiwan Ocean University, Keelung 20224, Taiwan

ARTICLE INFO

Article history:
Received 25 June 2010
Received in revised form 4 August 2010
Accepted 9 August 2010
Available online 19 August 2010

Keywords:
Characterization
Physical vapor deposition processes
Oxides

ABSTRACT

Nonpolar *a*-plane ZnO thin films were deposited on the single-crystal perovskite $SrTiO_3$ (1 0 0) substrates at 750 °C by radio-frequency magnetron sputtering. The effects of ultrathin 30 nm-thick ZnO buffer layer grown at 300–600 °C on the physical properties of ZnO/$SrTiO_3$(STO) thin films are investigated. A high growth temperature of ZnO buffer layer enhances not only the (1 1 0)-texture of ZnO/STO thin films but also the crystalline quality of the film. However, the ZnO/STO thin film without a ZnO buffer layer has a poor crystalline quality comparing to those with the ZnO buffer layer. Atomic force microscopy morphology studies reveal that the ZnO buffer layer largely decreases the surface roughness of the ZnO/STO thin films. This may be because of the thin ZnO buffer layer effectively decreases the stress between the ZnO and STO. The results of X-ray diffraction, high-resolution transmission electron microscopy, and photoluminescence spectra show that a high-quality epitaxial ZnO (1 1 0)/STO (1 0 0) thin film that emits UV light at room temperature can be formed with a thin ZnO buffer layer grown at 600 °C.

© 2010 Elsevier B.V. All rights reserved.

1. Introduction

ZnO is a wide-bandgap semiconductor with a very large exciton binding energy of 60 meV, which, in principle, allows the exciton-governed luminescence at short wavelengths to dominate at room temperature. ZnO has rapidly emerged as a promising optoelectronic material because of its potential usefulness in optoelectronic devices [1,2]. For many applications, ZnO epitaxial thin films with high crystalline quality are highly desirable [3]. Recently, the modulation of physical properties of perovskite oxide thin films by incorporating a ZnO oxide layer to form a heterostructure is proposed. The perovskites (ABO_3-type oxides) have remarkable physical properties and have potential in applications of novel devices [4–6]. A heterostructure that comprises perovskites and ZnO may exhibit versatile physical properties and support the evaluation of its possible applications in novel devices [7,8]. However, the synthesis of the heterostructures of perovskite oxide–wurtzite ZnO is still a challenge and the detailed studies on the structural information of the perovskite–wurtzite heterostructure are lacking.

$SrTiO_3$ (STO) is one of the mostly used substrates for the epitaxial growth of perovskite oxide thin films [6]. Understanding the growth characteristics of the ZnO thin films on the STO substrate is crucial for further integrating the perovskite oxides and wurtzite ZnO to fabricate devices with new functions. In general, a lattice misfit will exist between the different media due to the different lattice constants of the constituent compounds. This will cause strain in the film or induce many structural defects in the epitaxial thin films depending on film thickness. Recently, a low-temperature thin ZnO buffer layer was used to accommodate the lattice misfit strain in highly mismatched ZnO thin films that are grown on sapphire substrates [9]. Hence, understanding details of the structural information and evolution of ZnO grown on the perovskite materials with thin ZnO buffer layers are particularly important. This work systematically investigates the synthesis and structure of sputtering deposited ZnO thin films on STO substrates with a thin ZnO buffer layer grown at various temperatures.

2. Experimental

The ZnO/STO samples were fabricated by radio-frequency magnetron sputtering. Single-crystal STO with (1 0 0)-orientation was used as the substrates. STO substrates were cleaned with acetone and methanol and, then dried with N_2 gas. ZnO ceramic target with a purity of 99.99% was adopted to grow ZnO thin films. The ZnO film thickness is fixed at around 400 nm. The 30 nm-thick ZnO thin films grown at various temperatures (300–600 °C) were used as a buffer layer between the thick ZnO film and the STO substrate. During deposition for the 400 nm-thick ZnO film, the substrate temperature was fixed at 750 °C. The pressure of working gas during deposition of ZnO thin films was fixed at 5 mTorr with an Ar/O_2 ratio of 1:1 and the sputtering power density is fixed at 3.95 W/cm^2.

The crystallographic structures of ZnO/STO thin films were analyzed by measurements of high-resolution X-ray diffraction (XRD). The surface morphology of the ZnO thin films was investigated with an atomic force microscopy (AFM). Thin slices for analysis with a high-resolution transmission electron microscope (HRTEM) were prepared with a dual-beam focused-ion-beam instrument. The areas selected for cutting with an ion beam were protected with an amorphous carbon overlayer. The room temperature dependent photoluminescence (PL) spectra are obtained using the 325 nm line of a He–Cd laser.

E-mail addresses: yuanvictory@gmail.com, deanvera@yahoo.com.tw.

0925-8388/$ – see front matter © 2010 Elsevier B.V. All rights reserved.
doi:10.1016/j.jallcom.2010.08.037

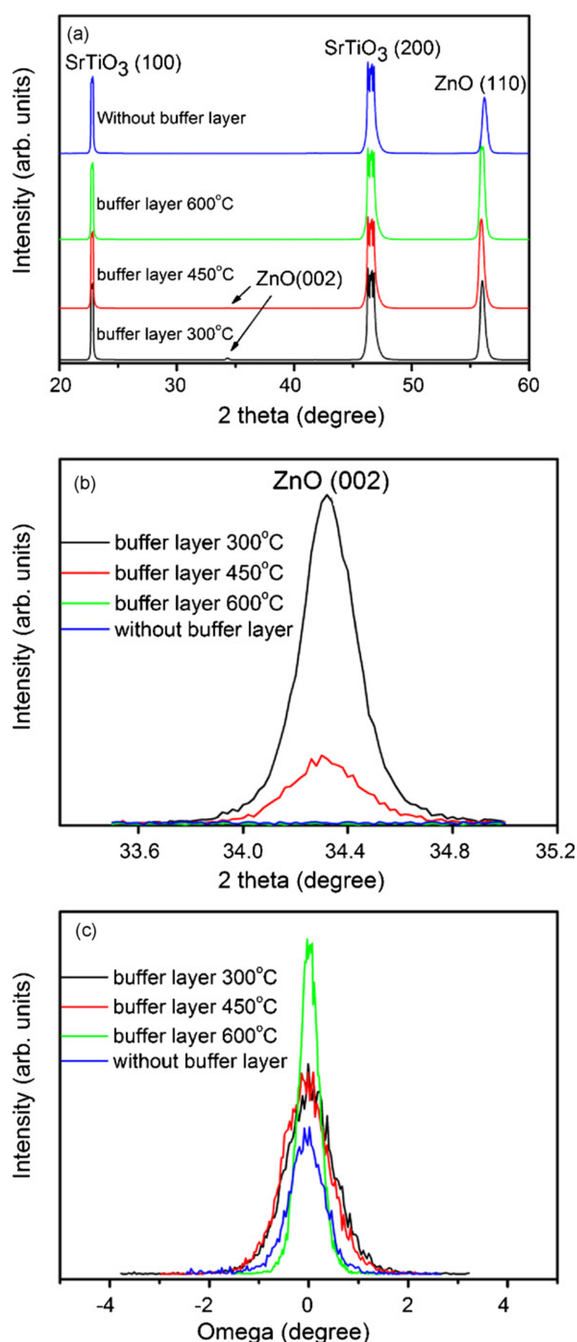

Fig. 1. (a) XRD patterns of ZnO/STO thin films with and without a ZnO buffer layer. (b) Magnified XRD patterns at the location of ZnO (0 0 2) Bragg reflections from ZnO/STO thin films. The ZnO/STO thin films without and with a ZnO buffer layer that was grown at 600 °C exhibit pure (1 1 0) Bragg reflections. (c) Rocking curves of the (1 1 0) Bragg reflection of ZnO/STO thin films with and without a ZnO buffer layer. The FWHM of ZnO/STO thin film without a ZnO buffer layer is 0.69°; those of ZnO/STO thin films with a ZnO buffer layer grown at 300 °C, 450 °C, and 600 °C are 0.98°, 0.92°, and 0.41°, respectively.

3. Results and discussion

Fig. 1(a) exhibits the XRD patterns of the 400 nm-thick ZnO/STO thin films without and with a thin ZnO buffer layer grown at various temperatures. The XRD patterns reveal a single wurtzite structure of ZnO and include well-defined (1 1 0) Bragg peaks from the ZnO thin films. The intensity of the (1 1 0) Bragg peak of ZnO thin films increases with growth temperature of the thin ZnO buffer layer. However, the (1 1 0) Bragg peak of the ZnO/STO thin film without a buffer layer has a relatively low intensity in comparison with that of ZnO/STO thin film having a ZnO buffer layer. A tiny (0 0 2) Bragg peak of ZnO was observed for the ZnO/STO films with a thin ZnO buffer layer grown below 600 °C, revealing these ZnO/STO thin films have mixed crystallographic characteristics. The content of (1 1 0)-oriented grains in the film can be roughly determined from the intensity ratio $I(1\,1\,0)/[I(0\,0\,2)+I(1\,1\,0)]$ of ZnO Bragg reflections. The background intensity was deducted from each Bragg reflection. The ZnO/STO thin films without and with a ZnO buffer layer that was grown at 600 °C exhibit pure (1 1 0) Bragg reflections. These ZnO/STO films have a pure (1 1 0)-oriented crystallographic feature. Moreover, the ZnO/STO thin films with a ZnO buffer layer grown at 300 and 450 °C have intensity ratios $I(1\,1\,0)/[I(0\,0\,2)+I(1\,1\,0)]$ of 96.2% and 98.1%, respectively, revealing a very small portion of (0 0 2)-oriented grains in the ZnO/STO thin films. A relatively low surface mobility of the atomic species during thin ZnO buffer layer deposition at a low-temperature might result in the formation of grains with mixed crystallographic features. This might account for the non-perfect (1 1 0)-oriented ZnO/STO thin films were formed with a ZnO buffer layer grown below 600 °C. The bulk ZnO has a hexagonal structure with lattice parameters $a = 0.3249$ nm and $c = 0.5206$ nm. The STO substrate is cubic with $a = 0.3905$ nm [6]. In ZnO (1 1 0)/STO (1 0 0) system, Karger and Schilling proposed that the lattice misfit in the ZnO film plane along the [−1 1 0] direction is ∼1.9% [10]. The lattice spacing of (1 1 0) Bragg reflection of the ZnO/STO thin films can be derived from Fig. 1(a). The lattice spacing of ZnO (1 1 0) plane for the ZnO/STO thin films with a ZnO buffer layer grown at various temperatures are the same (0.1641 nm). However, that of the ZnO/STO thin film without a ZnO buffer layer has a relatively small value of 0.1634 nm. The misfit between the ZnO and STO might cause a compressive strain in the ZnO film. The relatively small lattice spacing of (1 1 0) for the ZnO/STO thin film without a ZnO buffer layer might indicate that the ZnO buffer layer helps to release the lattice strain of thick ZnO film on the STO substrate. The use of buffer layer to reduce lattice misfit strain has been reported in ZnO thin films grown on sapphire or other single-crystalline substrates [9,11]. Fig. 1(c) plots the full widths at half maxima (FWHM) of (1 1 0) Bragg reflections from ZnO thin films. The FWHM value of ZnO (1 1 0) clearly decreases from 0.98° to 0.41° for the ZnO/STO thin films with the growth temperature of ZnO buffer layer increases from 300 to 600 °C. A ZnO buffer layer that was grown at a high growth temperature has a large grain size. This might decrease the density of nucleation sites and lowering the dislocation density for the subsequent deposition of ZnO thin film [12]. Moreover, a high temperature deposited ZnO buffer layer has a high degree of (1 1 0)-oriented grains in the film further enhancing not only the (1 1 0)-oriented feature of the ZnO/STO thin film but also its crystalline quality. In contrast, the FWHM of (1 1 0)-oriented ZnO/STO thin film without a ZnO buffer layer has a relatively large value (0.69°) comparing to that of the (1 1 0)-oriented ZnO/STO thin film with a ZnO buffer layer grown at 600 °C. The lattice strain may increase the mosaicity in the ZnO/STO thin film without a ZnO buffer layer [11]. The XRD analysis herein shows that a highly crystalline quality of (1 1 0)-oriented ZnO/STO thin film can be grown at a sufficiently high growth temperature of the ZnO buffer layer.

As depicted in Fig. 2, the epitaxial nature of the ZnO/STO thin film with a ZnO buffer layer grown at 600 °C is demonstrated by the in-plane orientations for (1 0 0) Bragg reflections of ZnO and (1 1 2) Bragg reflections of STO. No other peak is observable in intervals between these four peaks. This observation might be due to an existence of two kinds of growth domain perpendicular to each other in (1 1 0) ZnO grown on STO [13]. The same phenomenon has been observed in ZnO (1 1 0)/$LaAlO_3$ (1 0 0) system [14].

The TEM images of ZnO/STO thin film with a ZnO buffer layer grown at 600 °C was recorded with an incident electron beam

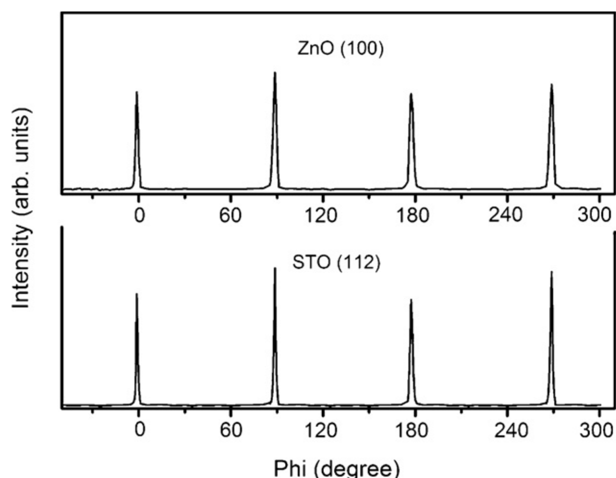

Fig. 2. Phi-scan curves of ZnO (1 0 0) and STO (1 1 2) reflections. The phi-scan profiles reveal satisfactory in-plane crystalline orientation of ZnO film with a thin ZnO buffer layer grown at 600 °C on the STO substrate.

parallel to ⟨1 1 0⟩ STO. Low-resolution cross-sectional TEM image (Fig. 3(a)) of ZnO epilayer on the STO reveals a dense crystalline film with no macroscopic imperfection; the total thickness of the ZnO layer was about 430 nm, conforming to the design value. Fig. 3(b) presents HRTEM image of the ZnO/STO interface showing the epitaxial growth of ZnO on the STO substrate. The interface of the ZnO/STO heteroepitaxy is atomically sharp; neither intermediate phase nor chemical reaction is observed at the interface.

Fig. 4 reveals the AFM surface images of ZnO/STO thin films with and without a ZnO buffer layer. The surface morphology of the ZnO/STO thin films with a ZnO buffer layer clearly shows an orthogonal domain structure. The epitaxial thin films of hexagonal $BaRuO_3$ on the STO (1 0 0) and nonpolar ZnO epilayer on the $LaAlO_3$ (1 0 0) show the same surface feature [14,15]. However, such an orthogonal domain structure was not observed in the epitaxial nonpolar Al-doped ZnO epilayer on the STO (1 0 0) [10]. The ZnO/STO thin film with a ZnO buffer layer grown at 600 °C has the lowest root-mean-square (rms) roughness of 4.06 nm. Moreover, the surface roughness of the ZnO/STO thin films with a ZnO buffer layer grown at 300–450 °C have rougher surface of 4.55–4.86 nm. The mixed crystallographic feature of the ZnO/STO thin films might result in a rougher surface structure than that of the (1 1 0)-oriented ZnO/STO [16]. In contrast, a quite rough surface structure that consists of large round grains was observed in the ZnO/STO thin film without a ZnO buffer layer, yielding an rms roughness of the film of 14.7 nm. The orthogonal domain structure of the ZnO/STO thin films might play an important role to release the strain induced by lattice misfit between the ZnO film and STO substrate. This can be confirmed from the XRD result that a relatively smaller spacing of (1 1 0) plane was found in the ZnO/STO thin film without a ZnO buffer layer.

The room temperature PL spectra of ZnO/STO thin films with and without a ZnO buffer layer are shown in Fig. 5. The main PL peak at about 3.26 eV is due to the free exciton emission in ZnO and a low energy shoulder is attributable to the emission related to point defects [2]. The emission efficiency is reported to be dependent on the crystalline degree of ZnO thin films [17]. The quality of ZnO thin films strongly influences the PL intensity ratio between the UV and visible emissions [18]. A very week defect-related visible emission was found in the ZnO/STO thin film with a ZnO buffer layer grown at 600 °C. A strong band edge emission peak with negligible defect-related visible emission has been reported on *c*-plane ZnO [19]. The atomic arrangements of the *c*-plane and *a*-plane ZnO are different. Both O and Zn atoms exist on the growing surface of *a*-plane ZnO. Therefore, native defects are energetically favorable and easier to form during the growth of ZnO (1 1 0) in comparison with that of ZnO (0 0 2) [20]. From Fig. 5, the relative PL intensity ratio of the dominant peak at ~3.26 eV increased with the growth temperature of ZnO buffer layer because a highly crystalline ZnO/STO thin film was formed with a ZnO buffer layer deposited at a high temperature. This result is consistent with the crystalline quality of ZnO/STO thin films from XRD patterns. Moreover, the rough surface structure and the distortion of ZnO lattice from the STO substrate might further increase the density of crystalline defects in the ZnO film without a ZnO buffer layer. This explains that a poor optical property of the ZnO/STO thin film without a ZnO buffer layer with respect to that of the ZnO/STO thin film with a thin ZnO buffer layer grown at 600 °C. The PL results show that a high-quality epitaxial (1 1 0)-oriented ZnO thin film that emits UV light at room temper-

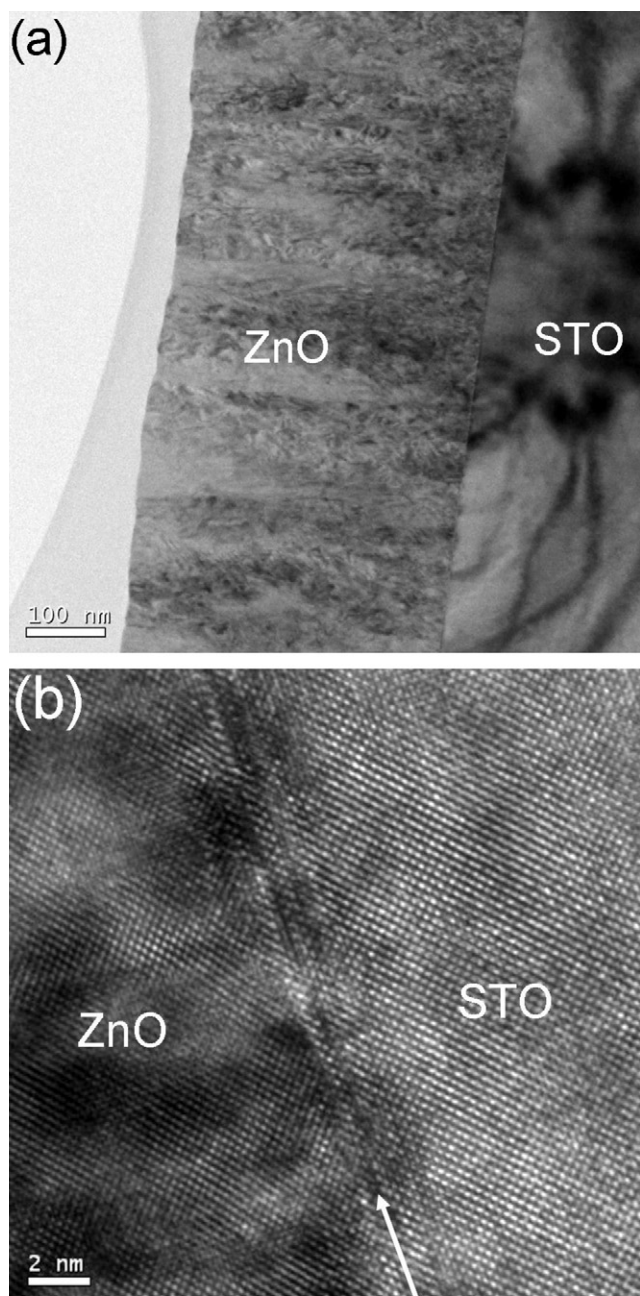

Fig. 3. (a) Cross-sectional TEM images at small magnification of ZnO/STO thin film with a ZnO buffer layer grown at 600 °C. (b) HRTEM image shows epitaxial growth of ZnO thin film on the STO substrate. Interface is marked with white arrows.

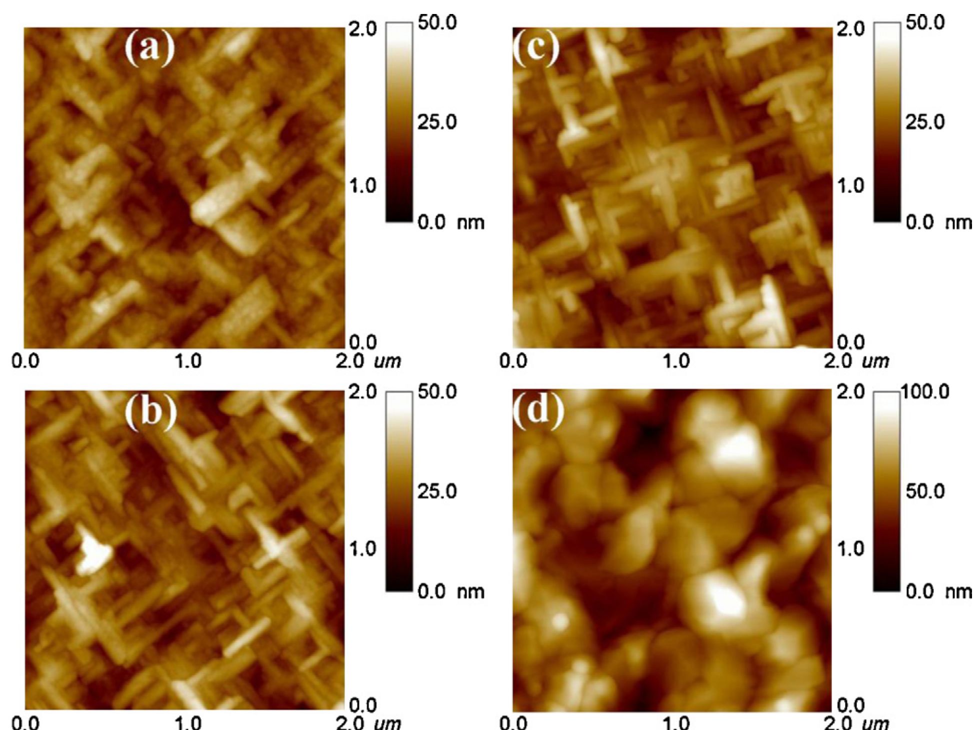

Fig. 4. Surface topography of ZnO/STO thin films with a ZnO buffer layer grown at (a) 300, (b) 450, (c) 600 °C, and (d) without a ZnO buffer layer.

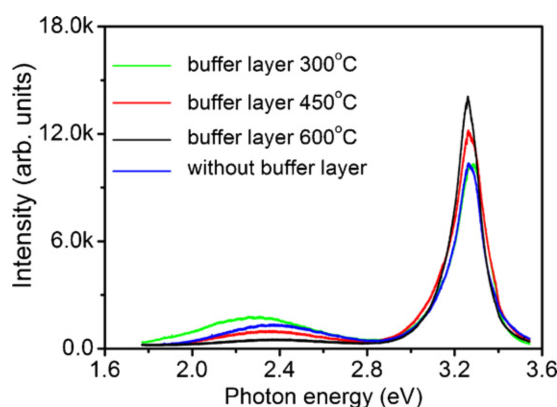

Fig. 5. PL spectra of ZnO/STO thin films with and without a ZnO buffer layer. PL intensity ratio between the UV and visible emissions increased with growth temperature of the ZnO buffer layer.

ature can be formed on STO substrate with a thin ZnO buffer layer grown at an adequate temperature.

4. Conclusions

The structural characteristics of highly mismatched ZnO/STO (1 0 0) thin films with and without a thin 30 nm-thick ZnO buffer layer were investigated using XRD, AFM, and HRTEM. The ZnO/STO thin films have a mixed crystallographic orientation when the ZnO buffer layer was grown at a temperature below 600 °C. Moreover, the ZnO/STO thin films grown without the buffer layer and with the ZnO buffer layer grown at 600 °C exhibit a (1 1 0)-oriented crystallographic feature. The crystalline quality of ZnO/STO thin films increases with the growth temperature of the ZnO buffer layer. The ZnO/STO thin film without the ZnO buffer layer exhibits the worst crystalline quality and the roughest surface structure among all the samples. Both structural analyses and PL results show that an epitaxial ZnO (1 1 0)/STO (1 0 0) thin film of high crystalline quality that emits UV light at room temperature can be formed with a ZnO buffer layer grown at 600 °C. The integration of high-quality epitaxial ZnO semiconductors with dielectric perovskite substrates may lead to the applications of novel optoelectronic devices.

Acknowledgements

The author would like to acknowledge the financial support from the National Taiwan Ocean University (Grant No. NTOU-RD-AA-2010-104031) and the National Science Council of the Republic of China (Grant No. NSC 99-2221-E-019-055).

References

[1] Y.C. Liang, C.C. Liu, C.C. Kuo, Y.C. Liang, J. Cryst. Growth 310 (2008) 3741.
[2] L. Wang, Y. Pu, W. Fang, J. Dai, Y. Chen, C. Mo, F. Jiang, J. Cryst. Growth 283 (2005) 87.
[3] Y.R. Ryu, A. Zhu, J.M. Wrobel, H.M. Jeong, P.F. Miceli, H.W. White, J. Cryst. Growth 216 (2000) 326.
[4] Y.C. Liang, Electrochem. Solid-State Lett. 12 (2009) G54.
[5] Y.C. Liang, Y.C. Liang, J.P. Chu, Electrochem. Solid-State Lett. 11 (2008) G41.
[6] Y.C. Liang, Y.C. Liang, J. Cryst. Growth 304 (2007) 275.
[7] A. Tiwari, C. Jin, D. Kumar, J. Narayan, Appl. Phys. Lett. 83 (2003) 1773.
[8] N. Ashkenov, M. Schubert, E. Twerdowski, H.V. Wenckstern, B.N. Mbenkum, H. Hochmuth, M. Lorenz, W. Grill, M. Grundmann, Thin Solid Films 486 (2005) 153.
[9] I.W. Kim, K.M. Lee, J. Appl. Phys. 103 (2008) 073514.
[10] M. Karger, M. Schilling, Phys. Rev. B 71 (2005) 075304.
[11] H.J. Ko, Y.F. Chen, Z. Zhu, T. Hanada, T. Yao, J. Cryst. Growth 208 (2000) 389.
[12] J. Han, T.B. Ng, R.M. Biefeld, M.H. Crawford, D.M. Follstaedt, Appl. Phys. Lett. 71 (1997) 3114.
[13] X.H. Wei, Y.R. Li, J. Zhu, W. Huang, Y. Zhang, W.B. Luo, H. Ji, Appl. Phys. Lett. 90 (2007) 151918.
[14] Y.T. Ho, W.L. Wang, C.Y. Peng, M.H. Liang, J.S. Tian, C.W. Lin, L. Chang, Appl. Phys. Lett. 93 (2008) 121911.
[15] M.K. Lee, C.B. Eom, J. Lettieri, I.W. Scrymgeour, D.G. Schlom, W. Tian, X.Q. Pan, P.A. Ryan, F. Tsui, Appl. Phys. Lett. 78 (2001) 329.
[16] Y.C. Liang, Ceram. Int. 36 (2010) 1743.
[17] M. Jung, J. Lee, S. Park, H. Kim, J. Chang, J. Cryst. Growth 283 (2005) 384.
[18] S. Bethe, H. Pan, B.W. Wesseis, Appl. Phys. Lett. 52 (1988) 140.
[19] A. Sasaki, W. Hara, A. Matsuda, N. Tateda, S. Otaka, S. Akiba, K. Saito, T. Yodo, M. Yoshimoto, Appl. Phys. Lett. 86 (2005) 231911.
[20] H.F. Liu, S.J. Chua, G.X. Hu, H. Gong, N. Xiang, J. Appl. Phys. 102 (2007) 083529.